Textile & Leather Review

ISSN 2623-6281| www.tlr-journal.com | 10.31881/TLR

Design of Functional Textile Fiber Materials for High-Performance Sportswear and Their Impact on Football Training Outcomes

Lei Wang

How to cite: Wang L. Design of Functional Textile Fiber Materials for High-Performance Sportswear and Their Impact on Football Training Outcomes. Textile & Leather Review. 2026; 9:56-79. https://doi.org/10.31881/TLR.2026.056

How to link: https://doi.org/10.31881/TLR.2026.056

Published: 20 January 2026

Design of Functional Textile Fiber Materials for High-Performance Sportswear and Their Impact on Football Training Outcomes

Lei WANG[1,2]

[1]Physical Education Department, Inner Mongolia University of Finance and Economics, Inner Mongolia, Hohhot 010070, China

[2]Graduate School of Education, Graduate University of Mongolia, Ulaanbaatar 14200, Mongolia

L_11_1984@163.com

Article

https://doi.org/10.31881/TLR.2026.056

Received 25 June 2025; Accepted 27 August 2025; Published 20 January 2026

ABSTRACT

The functionality of textile materials in high-performance sportswear significantly influences thermoregulation and muscle support during football training. This study presents a design approach focused on fiber microstructure and fabric integration to meet the combined demands of breathability, quick-drying, elasticity, and durability. Composite spinning and microstructural control techniques produced multi-interface, microporous fibers, applied in weft-knitted and layered fabrics. Testing achieved a moisture-vapor transmission rate of 11,320 g/(m²·24 h), a diffusion radius of 4.2 cm, an elastic recovery of 95.6%, and a low coefficient of friction (COF) of 0.37. The results from the training scenarios indicated improved regulation of the skin microclimate, reduced fatigue, and enhanced comfort. These results support the contribution of functional fibers in optimizing sportswear performance.

KEYWORDS

high-performance sportswear, functional fiber materials, textile structural design, thermal and moisture regulation, football training adaptation

INTRODUCTION

With the rising intensity of modern competitive sports, athletes demand higher comfort and functionality from sportswear. Traditional polyester or nylon fabrics exhibit limitations in key areas such as moisture permeability, quick drying, antibacterial properties, and elastic support, especially under high temperatures, humidity, and intense physical contact. These limitations hinder the body's dynamic stability and microclimate balance [1], leading to issues like sweat retention, heat buildup, and increased muscle tremors that impair energy distribution and performance [2,3]. The absence of structural optimization and insufficient fiber surface energy regulation in traditional fabrics result in poor sweat removal and air exchange [4,5]. Furthermore, under repeated stretching, friction, and washing, these materials degrade quickly and lack long-term stability [6,7]. To address this, a multi-dimensional functional fiber system is needed, integrating spinning control, structural optimization, and post-finishing treatment to enhance heat-moisture management, elastic support, and comfort [8,9].

This study develops functional fiber materials tailored for football training, starting with an analysis of thermoregulation, muscle stress, and frictional demands to define performance targets such as moisture permeability, elasticity, and durability. Using bicomponent spinning and microstructure control, fibers are constructed with microchannels, hydrophilic surfaces, and multi-interface composites. Fabrics are formed via weft and warp knitting, optimized by load zones and treated for antibacterial and moisture-regulating functions. Standardized tests and simulation devices assess material–body interactions, including moisture transfer, tensile deformation, dynamic friction, and contact pressure. Field tests in training scenarios evaluate adaptability through physiological data, microclimate tracking, and subjective feedback. This work establishes a quantifiable relationship between textile design, functional integration, and athlete response, addressing the gap in modeling the interaction between fabric parameters and sports performance.

RELATED WORK

In recent years, researchers have conducted systematic research on functional fiber materials for sportswear from the perspective of structural optimization and multifunctional integration. Atallah H A A et al. [10] improved the thermal comfort of clothing in low-temperature environments through multilayer structures and controllable ventilation design; Dolez P I et al. [11] summarized the application potential of high-extension elastic fibers and high-performance polymers in protective equipment; Gulati R et al. [12] analyzed the stability and practical advantages of antimicrobial agents in textiles. The above studies mostly focus on single-function optimization and lack multifunctional integration verification in actual sports scenarios.

Ioannou L G et al. [13] compared the effects of different tops on athlete performance and found that cotton and aluminum-coated clothing had poor local cooling; Zhao X [14] developed smart sportswear based on nanomaterials with excellent moisture management, ultraviolet (UV) protection and thermal control performance; Cheng P et al. [15] pointed out that heat and moisture exchange and mechanical constraints are key factors affecting the comfort of tight-fitting clothing, especially in the waist, chest and lower limb areas. Despite progress in material performance and user feedback, current research still lacks a systematic integration of material properties, physiological responses and football-specific needs, and multi-dimensional functional matching still needs to be improved.

METHODS

Performance Requirements of Sportswear in Football Training Environment

In the analysis of sportswear performance requirements in the football training environment [16], this study systematically collects climate parameters and athlete physiological load data in high-intensity football training scenes to construct a multi-dimensional clothing functional requirements model. This study was approved by the Ethics Committee of Inner Mongolia University of Finance and Economics. All participants provided informed consent prior to the study.

To ensure the quantifiable expression of performance indicators, the study applies the permeability (P) calculation equation commonly used in textile engineering [17,18]:

$$P = \frac{V}{A \cdot t \cdot \Delta p} \tag{1}$$

where P represents the air permeability; V represents the volume of air passing through the fabric per unit time (m³); A represents the test area (m²); t represents time (s); and Δp represents the pressure difference (Pa). This parameter is used to evaluate the demand for air circulation capacity of sportswear under different training intensities and serves as an important basis for the subsequent design of functional fiber structures.

Air permeability tests were conducted under standard atmospheric conditions using a fabric air permeability tester compliant with ISO 9237. The pressure differential was set at 100 Pa over a test area of 20 cm². Once airflow stabilized, the volume of air passing through the sample per unit time was automatically recorded. The time was captured by the instrument's built-in timing system, and the pressure differential was monitored and maintained constant in real time by a high-precision pressure sensor. All samples were conditioned for 24 hours at a standard temperature and humidity before testing to ensure the stability and comparability of the test data.

For moisture absorption and diffusion performance, the moisture conduction rate model based on the capillary action principle is used to describe it, and its mathematical expression is as follows:

$$D = \frac{r^2}{4\eta t} \ln\left(\frac{L}{r}\right) \tag{2}$$

where D is the diffusion coefficient (m²/s); r is the fiber capillary radius (m); η is the liquid viscosity (Pa·s); L is the capillary length (m); and t is time (s). This model is used to guide the design direction of the fiber microporous structure so that the fabric has a more efficient sweat migration ability.

In the corresponding analysis of the training load and body support requirements, the theoretical calculation model of the fabric elastic recovery rate (ERR) is applied:

$$ERR = \frac{\varepsilon_0 - \varepsilon_r}{\varepsilon_0} \times 100\% \tag{3}$$

where ε_0 is the initial tensile strain (%), and ε_r is the residual strain after release (%). The model is used to derive the specific requirements of clothing elasticity for different training movements, and the arrangement and content ratio of the two-component fibers in the fabric structure are set accordingly.

Elastic recovery tests were conducted on a universal testing machine with a set tensile rate of 100 mm/min. The strain was maintained for 30 s before unloading to zero. After 5 minutes of rest, the residual strain was measured. The initial strain was precisely controlled by the clamping distance, and the residual strain was automatically measured via the machine's displacement sensor. Each sample was tested five times to ensure data repeatability and reliability.

To characterize the friction response behavior of the fabric surface, a calculation model for the coefficient of friction (COF) of the fabric surface based on the Amontons–Coulomb friction law is established:

$$\mu = \frac{F_f}{F_n} \tag{4}$$

where F_f is the friction force (N) and F_n is the normal load (N). This parameter is used to guide the selection of finishing processes to reduce the sliding resistance between the fabric and the skin and improve wearing comfort.

The data analysis used principal component analysis (PCA) to reduce the dimensionality and to extract air permeability, moisture-diffusion radius, ERR and COF as core variables, and construct a functional response matrix to characterize the thermal and moisture regulation, moisture transfer, mechanical support and contact comfort [19,20]. Through factor weight and cluster analysis, the performance demand differences in different training stages and body parts were identified.

Based on the statistical results, the demand intensity of each indicator in different parts was scored on a scale of 1-5. Table 1 lists the main demand level distributions of air permeability, elastic support and moisture diffusion.

Table 1. Demand intensity level distributions of key performance indicators in each body area

Body Region	Air Permeability Demand	Elastic Support Demand	Moisture Diffusion Demand
Upper Back	4	2	5
Lower Thigh	3	5	3
Abdomen	2	3	4

Knee Area	3	4	2
Upper Arm	5	2	4

As shown in Table 1, different parts of the body have different functional requirements for fabrics during football training: the upper back requires high breathability and moisture management, with low elasticity requirements; the lower thigh emphasizes high elastic recovery to stabilize the muscle group, with moderate hygroscopicity; the abdomen needs to balance moisture transfer and elasticity; the knee joint requires high structural elasticity to cope with flexion and shear stress; and the upper arm focuses on breathability and moisture conduction, with lower mechanical support requirements.

On this basis, a regression model based on fabric structural parameters and performance indicators is further established, and its general form is as follows:

$$y = \beta_0 + \beta_1 x_1 + \beta_2 x_2 + \cdots + \beta_n x_n + \varepsilon \tag{5}$$

where y represents a certain performance indicator, such as moisture vapor transmission rate (MVTR) or ERR; $x_1, x_2, \ldots, x_n$ represents independent variables such as the fiber diameter, yarn density, and tissue structure parameters; $\beta_0, \beta_1, \ldots, \beta_n$ represents regression coefficients; and ε represents the error term.

A dynamic motion capture system is used to synchronously record the temperature and humidity changes of athletes in typical football actions such as simulated confrontation, sprinting and change of direction. The local moisture permeability differences and moisture conduction needs are quantified by combining biomechanical parameters such as the hip joint rotation angle and lower limb muscle contraction frequency.

Structural Design and Spinning Scheme of Functional Fiber Materials

In response to the requirements of football training uniforms for moisture permeability, elastic recovery and friction control, polyester fibers with hollow channels, microporous structures and hydrophilic surfaces were prepared via two-component composite spinning and microstructure control technology [21,22]. By regulating the melt phase separation and interface effect, the controllable construction of the internal microstructure of the fiber is achieved, and the thermal and moisture management and mechanical properties are improved.

With high-viscosity poly(ethylene terephthalate) (PET) as the core layer and low-viscosity modified polyester as the surface layer, a special-shaped cross-section is formed in conjugate spinning. By adjusting the component ratio and the difference in extrusion rate, non-uniform cooling shrinkage is induced to construct an axial microchannel network. The process is based on rheological analysis and combined with the constitutive equation of a generalized Newtonian fluid for simulation optimization:

$$\tau = K \cdot \dot{\gamma}^n \tag{6}$$

where τ is the shear stress; $\dot{\gamma}$ is the shear rate; K is the consistency coefficient; and n is the flow index, which is used to describe the flow characteristics of the polymer melt in the spinneret during spinning and to optimize the combination of the spinning temperature and drawing speed parameters accordingly.

In order to improve the moisture absorption and moisture conduction performance of the fiber, the cortical hydrophilic group modification technology is used to introduce a third monomer containing sulfonate to build a continuous hydrophilic interface on the fiber surface, regulate the surface polarity and tension, and enhance the adsorption and diffusion of sweat molecules. Combined with online electrostatic charging technology, a directional dipole structure is induced under a high-voltage electric field to further reduce the contact angle and improve wettability. An interfacial tension model is established based on the Young–Laplace equation to analyze the surface wetting behavior:

$$\Delta P = \gamma \left(\frac{1}{R_1} + \frac{1}{R_2}\right) \tag{7}$$

where ΔP is the pressure difference on both sides of the interface; γ the surface tension; R_1 and R_2 the curvature radii, which are used to guide the fiber surface morphology regulation and wetting performance optimization.

In the stabilization of fiber structure, gradient crystallization-orientation coupling technology is used to optimize the orderly arrangement of the crystalline and amorphous regions inside the fiber by regulating the heat setting temperature and stretching multiple, thereby improving the dimensional stability and durability. This process combines thermodynamic and kinetic control mechanisms to achieve structural regulation based on the Arrhenius relationship between crystallinity and temperature:

$$ln\ \left(\frac{dX}{dt}\right) = ln\ A_1 - \frac{E_a}{RT} \tag{8}$$

where X is the crystallinity; t the time; A_1 the pre-exponential factor; E_a the activation energy; R the gas constant; and T the absolute temperature, which is used to analyze the evolution of the fiber structure under different heat treatment conditions.

Figure 1 shows the structure of the two-component spinning system, clearly showing the melt distribution path and cooling solidification area during the formation of the core–skin structure.

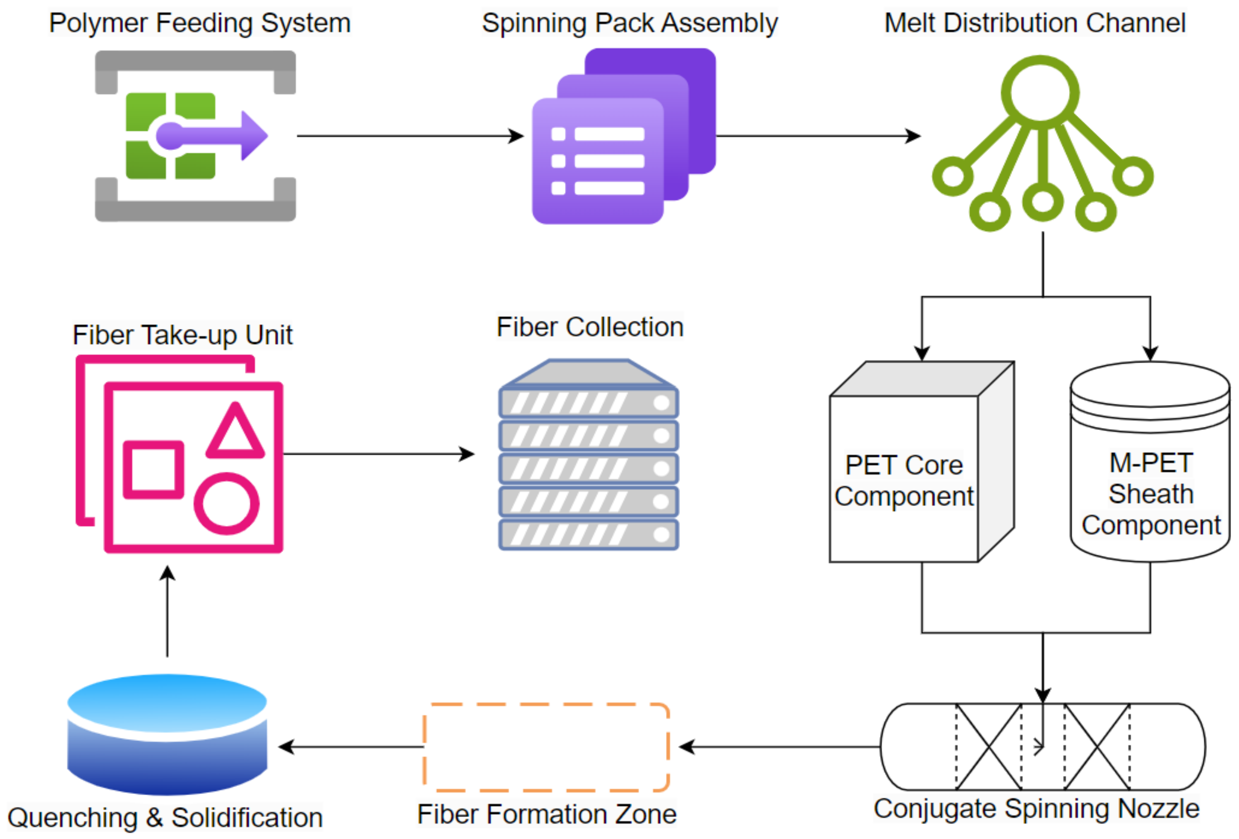

Figure 1. Schematic diagram of the two-component spinning system and the formation of the cross-sectional structure

Figure 1 shows the structure of the two-component spinning system and the process of forming the core–skin structure. The system includes polymer supply, spinning assembly, melt channel and composite spinneret, and is equipped with a cooling zone. During spinning, high-viscosity PET and low-viscosity modified polyester are temperature-controlled and regulated separately to form a parallel composite structure in the channel, which is extruded through the spinneret and then cooled and solidified. During stretching, axial microchannels are formed due to the difference in component shrinkage. By regulating the spinning temperature, cooling airflow and stretching tension, stable fibers with controllable structure and hydrophilic surface can be obtained, which are suitable for high-performance knitting and multilayer fabrics.

Fabric Construction Scheme for Differences in Wearing Areas

Based on the stress distribution and sweating characteristics of various parts of the body during dynamic movement, regional fabric design is adopted. For high tensile load areas (such as the trunk and proximal limbs), a double-rib weft-knitted structure with asymmetric coil arrangement is designed to improve elasticity and multi-axial adaptability. High-elastic double rib structure is used to support muscles in key parts of the lower limbs, and a multilayer composite structure is used in the trunk to enhance stability and thermal regulation performance. The warp and weft gradient mechanical response is achieved by alternating high and low modulus yarns. The Mohr–Coulomb constitutive equation is improved to simulate the stretch recovery behavior of the fabric:

$$\sigma_{ij} = \sum_{k=1}^{n} C_{ijkl}\varepsilon_{kl} + \alpha \frac{\partial \varepsilon_{kl}}{\partial t} \tag{9}$$

where σ_{ij} represents the stress tensor; C_{ijkl} is the stiffness coefficient matrix; ε_{kl} is the strain tensor; and α is the viscoelastic correction coefficient. The model reveals the relationship between the energy dissipation mechanism and the structural recovery ability of fabrics in dynamic stretching. In the implementation, the double-sided circular knitting machine needle selection mechanism is used to accurately embed functional yarns to construct three-dimensional periodically interwoven wicking moisture-conducting channels and elastic support units.

For high-frequency bending areas such as knee joints and scapulae, a biaxial warp-knitted multilayer composite structure is used, and a directional support yarn layer is superimposed on the base fabric through a multi-comb device to achieve structural enhancement and deformation adaptability. The functional layers are mechanically connected through the spacer fabric technology, and the interlayer shear stiffness G can be estimated by the following empirical equation:

$$G = \frac{N \cdot d \cdot \sin\theta}{h} \tag{10}$$

where N is the number of crossed yarns per unit area; d the yarn diameter; θ the interlayer yarn deflection angle; and h the interlayer spacing. The structure effectively improves the anti-buckling performance by adjusting the yarn deflection angle and interlayer density while maintaining good moisture permeability. The electronic warp feeding system is used in weaving to independently control the tension of each layer to achieve coordinated deformation of the functional layer. In the sweat concentration area, a unidirectional moisture-conducting layer of fibers with specially shaped cross-sections is designed, and its capillary action is determined according to the improved Washburn equation:

$$L_1 = \frac{r\gamma\cos\theta_1}{2\eta}\sqrt{\frac{t}{\rho}} \tag{11}$$

where L_1 is the liquid climbing height; r the characteristic radius of the fiber cross section; γ the surface tension; θ_1 the contact angle; η the liquid viscosity; t the time; and ρ the liquid density. This parameter guides the optimal design of the fiber cross-sectional profile, so that the moisture-conducting layer forms a directional moisture migration path in the weft-knitted ground structure. At the same time, a phase change thermoregulating fiber layer is embedded in the multilayer composite structure, and its thermal response characteristics are described by the crystallization kinetics Avrami equation:

$$X(t) = 1 - \exp\left(-Kt^n\right) \tag{12}$$

where $X(t)$ is the rate of change in crystallinity with time; K the crystallization rate constant; and n the Avrami index. This model is used to predict the phase change endothermic behavior of fibers under body temperature stimulation, thereby optimizing their thermal regulation efficiency during intense exercise.

In the fabric splicing area, the seamless pressing technology is used to achieve the continuous transition of different structural units. The stress concentration coefficient β at the seam can be predicted by finite element simulation:

$$\beta = \frac{\sigma_{max}}{\sigma_{nom}} \tag{13}$$

where σ_{max} is the maximum principal stress in the seam area, and where σ_{nom} is the nominal stress.

Fabric Finishing and Functional Enhancement Treatment

In the process of fabric finishing and functional enhancement, in order to meet the comprehensive requirements of durability, comfort and functional stability of high-performance sportswear, a multi-step collaborative process is used to systematically modify the fiber material [23,24]. First, low-pressure radio frequency plasma technology is used to excite high-energy ion beams in a mixed atmosphere of argon and oxygen to activate the fiber surface, introduce uniformly distributed free radical sites without damaging the bulk structure, improve its polarity and reactivity, and provide a good interface foundation for subsequent chemical grafting. The change in surface energy can be quantified by contact angle measurement based on the Young–Dupré equation:

$$\cos\,\theta_1 = \frac{\gamma_{\mathrm{S}} - \gamma_{\mathrm{SL}}}{\gamma_{\mathrm{L}}} \tag{14}$$

where γ_{S} is the solid surface tension; γ_{SL} the solid–liquid interface tension; γ_{L} the liquid surface tension; and θ_1 the contact angle. By adjusting the plasma treatment time and power density parameters, the contact angle is reduced to below 30°, thereby enhancing the fiber's adsorption capacity for subsequent functional additives.

The nanosilver particles were embedded in the fiber micropores by in-situ silver ion complex deposition. First, the fabric was immersed in a thiol-containing coupling agent solution to form a thiol-metal coordination anchoring layer, and then silver nanoparticles with a particle size of 20–50 nm were generated on its surface through a two-step reduction process. This process involves a charge transfer kinetic mechanism, and its deposition rate can be described by the Butler–Volmer equation:

$$j = j_0\left[exp\left(\frac{\alpha_a F}{RT}\eta\right) - exp\left(-\frac{\alpha_c F}{RT}\eta\right)\right] \tag{15}$$

where j is the current density; j_0 the exchange current density; α_a and α_c the anode and cathode transfer coefficients, respectively; F the Faraday constant; R the gas constant; T the thermodynamic temperature; and η the overpotential. By controlling the reducing agent concentration gradient and the reaction temperature, a uniform distribution of silver particles on the fiber surface can be achieved, avoiding the problem of decreased antibacterial efficacy due to local aggregation.

In the optimization of antistatic performance, a polyether ester permanent antistatic agent is used for cross-linking treatment so that its molecular chain is embedded in the amorphous area of the fiber to construct a continuous conductive channel. By adjusting the ratio of antistatic agent to cross-linking agent, the functional component is prompted to form a covalent bond with the fiber macromolecule under high temperature baking, thereby improving the washing fastness. The antistatic effect is reflected by the volume resistivity ρ_v, which is expressed as follows:

$$\rho_v = R_v \cdot \frac{A_2}{d_1} \tag{16}$$

where R_v is the measured volume resistivity (Ω); A_2 the effective area of the electrode (m²); and d_1 the sample thickness (m).

To improve the softness and humidity control performance, silicone-based organic modified amino silicone oil is used for surface lubrication treatment. By controlling the emulsion particle size distribution and osmotic pressure difference, the silicone oil droplets are evenly covered on the fiber surface without blocking the microporous structure. This process combines mechanical kneading and heat setting processes to improve the touch properties while maintaining the original air permeability of the fabric. The surface COF μ of the treated fabric was calculated via the following equation:

$$\mu = \frac{F_1}{P_n} \tag{17}$$

where F_1 is the sliding friction force (N) and P_n is the vertical load (N). By adjusting the ratio concentration of the silicone oil emulsion and the heat treatment temperature, the fiber surface COF can be adjusted to the optimal range, thereby improving the smoothness of the clothing in dynamic sports scenes.

Structural Garment Design and Sample Production of High-Performance Sportswear

In designing high-performance football training uniforms, a regional structural strategy is applied based on athletes' dynamic demands. Stress distribution and perspiration patterns guide the differentiated configuration of weft-knitted elastic and multilayer composite fabrics across the trunk, limbs, and joints. 3D body scanning and CAD modeling enable digital design and virtual fitting to optimize the fabric tension distribution, whereas hot-press fusion ensures seamless splicing at the shoulders and waist for improved comfort and aerodynamics.

During cutting, fabric rebound is calculated using the Mohr–Coulomb constitutive equation to ensure fit [25,26]. This equation is used to describe the deformation recovery behavior of a material after stress release. By introducing an empirical yield criterion, the fabric rebound is estimated to optimize the cutting allowance design and improve garment fit accuracy. A biaxial warp-knitted composite structure is used at the knees and elbows with reserved wrinkle margins for mobility. The orientation of special-shaped fibers is determined via the improved Washburn equation to enhance moisture conduction. Ultrasonic welding enables needleless seams, improving seam strength and the accuracy of stress distribution, whereas high-modulus yarns embedded in the waist and outer thighs enhance support. The stitching materials and stitch density are optimized based on friction mechanics to reduce slippage risk.

After garment completion, a dummy heat–humidity system evaluates microclimate control. Infrared thermal imaging and breathability models assess temperature and humidity regulation, while dynamic tensile tests verify elastic recovery and muscle tremor suppression. Test data inform structural parameter optimization, balancing performance and comfort.

EXPERIMENTS

Preparation of Experimental Materials and Devices

The experimental platform was established a comprehensive fabrication and characterization system for functional fiber materials. A two-component melt-spinning unit was used to achieve precise blending of PET and modified polyester, with independent temperature control, multi-channel distribution and online diameter monitoring (100 Hz) to ensure stable molding. Weaving uses double-sided circular knitting machines and multi-comb warp knitting machines: the circular knitting machine selects needles to embed moisture-conducting high-modulus yarns, and the warp knitting machine regulates the interlayer tension through electronic warp feeding to build a structurally controllable weft-knitted elastic and warp-knitted multilayer composite structure. Finishing includes plasma activation, silver ion deposition and antistatic treatment: in an argon–oxygen atmosphere; silver ions are uniformly deposited after pretreatment, reduction, and fixation; and antistatic agents are cured at high temperature to form covalent bonds to improve washability. The performance tests cover wet heat, stretching, friction and breathability: dynamic hygroscopicity, stress–strain elasticity and shock suppression effects, sliding friction comfort, and breathability are all quantitatively evaluated.

To ensure data traceability, a spinning parameter comparison table is formulated, covering key variables such as core/skin temperature, drawing speed, cooling wind speed and final fiber diameter, as the basis for subsequent analysis and optimization.

Control Group A comprises commercial polyester fibers for sportswear, produced under standard melt-spinning conditions. Control Group B uses identical raw materials but with a reduced draw ratio and slower cooling, resulting in structural inhomogeneity. These groups serve as reference points to evaluate the improvements from optimized processing in the experimental group.

Table 2 lists the physical properties of the functional fibers obtained under different spinning parameters, including the processing temperature, drawing speed, cooling wind speed, and final fiber diameter of the core layer (PET) and skin layer (modified polyester). The PET core layer temperatures were maintained at 290°C, 295°C, and 300°C with corresponding skin layer temperatures of 275°C, 280°C, and 285°C, respectively. These temperature gradients controlled viscosity differentials to achieve a stable interfacial morphology and uniform phase distribution. The drawing speed was set to 800, 850, and 900 m/min, and the cooling wind speed was set to 0.6, 0.7, and 0.8 m/s to control the solidification rate and orientation structure. The results showed fiber diameters of 22.3, 21.8, and 21.5 μm, respectively, indicating that with increasing temperature and drawing rate, the fiber thinning trend was obvious, the diameter fluctuation was small, and the process consistency was good. The diameters obtained in repeated experiments for control groups A and B were 24.1 μm and 23.6 μm, respectively, reflecting high system repeatability and stability. All diameter data were collected using a laser diameter meter at 100 Hz to ensure data continuity and representativeness.

Table 2. Physical parameters of fibers under different spinning conditions

Spinning Parameters	PET Core Temperature (°C)	Low Viscosity Modified Polyester Skin Layer Temperature (°C)	Drawing Speed (m/min)	Cooling Wind Speed (m/s)	Fiber Diameter (μm)
Experimental Group1	290	275	800	0.6	22.3
Experimental Group2	295	280	850	0.7	21.8
Experimental Group3	300	285	900	0.8	21.5
Control Group A	290	275	800	0.6	24.1
Control Group B	295	280	850	0.7	23.6

Fabric Physical Properties and Heat and Moisture Regulation Ability Test

During the experimental testing phase, standardized methods were used to systematically evaluate the physical properties and thermal and moisture regulation properties of the prepared functional fiber materials. Key indicators such as air permeability, MVTR, moisture diffusion radius, ERR and friction coefficient were used to evaluate its applicability in football training.

The wet heat simulator records moisture transfer and thermal resistance under different climates; the multi-directional tensile test obtains stress–strain response and elastic recovery to evaluate the muscle tremor suppression effect; the sliding platform measures the friction coefficient of simulated skin contact to evaluate comfort. All samples were pretreated to equilibrium moisture content at standard temperature and humidity, and the test covered static and dynamic conditions.

The air permeability was calculated using the airflow resistance model, the MVTR was determined by the 24-hour gravimetric method, the wicking test evaluated the liquid diffusion capacity, the ERR was calculated based on the residual deformation, and the friction coefficient was determined by the relationship between the sliding force and the normal load.

Table 3 shows the test results of the air permeability, MVTR, moisture diffusion radius, ERR and friction coefficient, and combined with the changes in the spinning process parameters, reveals the relationship between the material structure and performance.

Table 3. Key performance test data of the functional fiber fabrics

Spinning Parameters	Air Permeability ($m^3 \cdot m^{-2} \cdot s^{-1}$)	Moisture Vapor Transmission Rate ($g/(m^2 \cdot 24\ h)$)	Moisture Diffusion Radius (cm)	Elastic Recovery Rate (%)	Coefficient of Friction
Experimental Group1	38.6	11,320	4.2	95.6	0.37
Experimental Group2	37.9	10,980	4.0	94.8	0.38
Experimental Group3	36.4	10,650	3.9	93.5	0.39
Control Group A	35.1	10,320	3.7	92.1	0.40
Control Group B	34.2	9,980	3.6	91.3	0.41

Table 3 presents the key performance data of functional fiber fabrics under different processing conditions. All the measurements were conducted under standardized climate conditions after sample conditioning. The test items include the air permeability, MVTR, moisture diffusion radius, ERR, and COF. These parameters serve as the baseline dataset for subsequent analysis in Section 5.

Table 4 systematically presents the statistical results of the intergroup differences in key performance indicators between the experimental group and the two control groups, including the mean difference, standard deviation, p-value, and significance mark for the water evaporation rate, moisture conduction radius, ERR, and friction coefficient. Significance levels of $p < 0.05$ are marked with *, $p < 0.01$ with **, and p

< 0.001 with ***.

Table 4. Statistical analysis of intergroup differences in key performance indicators of functional fiber fabrics

Performance Indicator	Group Comparison	Mean Difference	Standard Deviation	p-value	Significance Level
Moisture Vapor Transmission Rate (g/(m²·24 h))	Experimental vs. Control A	1,020	142.3	0.003	**
	Experimental vs. Control B	1,340	158.7	<0.001	***
Moisture Diffusion Radius (cm)	Experimental vs. Control A	0.4	0.06	0.008	**
	Experimental vs. Control B	0.6	0.08	<0.001	***
Elastic Recovery Rate (%)	Experimental vs. Control A	3.2	0.41	0.002	**
	Experimental vs. Control B	4.3	0.53	<0.001	***
Coefficient of Friction	Experimental vs. Control A	-0.02	0.003	0.012	*
	Experimental vs. Control B	-0.03	0.004	<0.001	***

Football Training Wear Experiment and Training Effect Evaluation

The experimental sportswear was evaluated during standardized football training tasks [27], collecting physiological and performance data including heart rate, skin temperature and humidity, subjective fatigue scores, and movement execution quality, then comparing with baseline data to analyze its training impact.

A cohort of 20 male collegiate football players, aged 20–24, with a minimum of five years of competitive training experience and body fat percentages between 12% and 16%, participated in the study. The trial followed a randomized, controlled, crossover design, with participants completing two identical high-intensity training protocols separated by a seven-day washout period, wearing either the experimental garment or a control garment matched in mass, thickness, and baseline stretch. Testing was conducted in a climate-controlled environment maintained at 25°C and 55% relative humidity. Participants adhered to standardized pre-test conditions regarding diet, sleep, and physical activity 48 hours prior to each session. Physiological monitoring included continuous heart rate telemetry, real-time skin temperature and humidity measurements at multiple anatomical sites, and surface electromyography of lower limb muscles. Subjective fatigue was assessed using a validated numeric rating scale administered before and after each session.

The 3D motion capture system recorded the joint angular velocity and limb acceleration during sprinting and cutting maneuvers. The data were processed to derive stride frequency, contact time, and movement consistency indices. Surface electromyography (EMG) signals from lower limb muscles were analyzed for activation timing and co-contraction ratios, reflecting neuromuscular control under fatigue. These kinematic and electrophysiological parameters were synchronized with skin microclimate data to assess the garment's influence on movement stability and technical execution throughout the training session.

Sprint speed and blood lactate concentration were recorded and combined with physiological and kinematic data to build a comprehensive evaluation model assessing how the garment improves movement efficiency. Change-of-direction speed, shooting accuracy, sprint performance, and blood lactate fluctuations were also monitored to quantify functional benefits. In a controlled environment, athletes performed continuous high-intensity tasks—sprints, directional changes, simulated confrontation, and endurance runs—under consistent conditions. Wireless systems recorded real-time heart rate, and wearable skin sensors captured microclimate data. Subjective fatigue and movement quality scores were gathered pre- and post-training to assess adaptability.

The subjective fatigue score was assessed using a standardized numeric rating scale ranging from 1 to 20, where 1 indicated no sensation of fatigue and 20 represented maximal perceived exertion.

This scale was developed based on psychophysical principles of perceived exertion and adapted for sport-specific contexts requiring finer gradation in high-intensity intermittent exercise. The linear range from 1 to 20 allows enhanced sensitivity in tracking fatigue progression during dynamic football training, with clear anchor points established through pilot testing to ensure consistent interpretation across participants.

Athletes were instructed to evaluate their overall physical fatigue level based on muscular strain, movement effort, and endurance depletion. The assessment was conducted immediately before and after each training session under standardized conditions to ensure consistency.

EMG measured lower limb muscle activity to analyze the elastic support structure's effect on muscle tremor, while a 3D motion capture system tracked joint angles and limb trajectories to evaluate movement stability. Based on these data, a regression model relating training intensity to physiological response was established to quantitatively describe the relationship between clothing performance and athletic output [28].

Table 5 shows the changes in key physiological and kinematic parameters at different training stages, reflecting the role of clothing in maintaining physiological stability and relieving muscle fatigue.

Table 5. Changes in the physiological and kinematic parameters of athletes at different training stages

Training Phase	Heart Rate (bpm)	Skin Temperature (°C)	Skin Humidity (%RH)	EMG Amplitude (mV)	Fatigue Score
Initial	118	32.4	58	0.32	9
Mid	142	34.7	76	0.58	14
Final	165	36.9	89	0.87	18

Table 5 shows that athletes' skin humidity rose significantly during training, indicating increased sweat secretion. The experimental clothing must maintain good moisture permeability and conduction under high humidity to prevent discomfort. The gradual increase in electromyographic signal amplitude reflected accumulating muscle fatigue, suggesting that the elastic support structure helps alleviate fatigue development. Fatigue score trends also confirmed this, with subjective fatigue rising over training time.

Overall, these data verify the effectiveness of functional fiber materials in enhancing sportswear performance and provide a basis for future optimization.

RESULTS

Test Results of Fabric Moisture Permeability and Moisture Conduction Performance

Systematic variation of spinning parameters influenced the microchannel architecture and surface hydrophilicity, thereby modulating the moisture transfer behavior. With increasing temperature and drawing rate, the reduction in MVTR and diffusion radius indicates a denser internal structure and enhanced capillary continuity, which promotes directional moisture conduction rather than isotropic permeability. Five sample groups (three experimental and two control groups) were established to represent fiber-forming conditions under varying core/surface polymer temperatures, drawing speeds, and cooling wind speeds. The test indicators included MVTR, reflecting sweat evaporation efficiency, and the moisture diffusion radius, indicating lateral moisture conduction of liquid water. Figure 2 shows the trends of these indicators with changing spinning parameters.

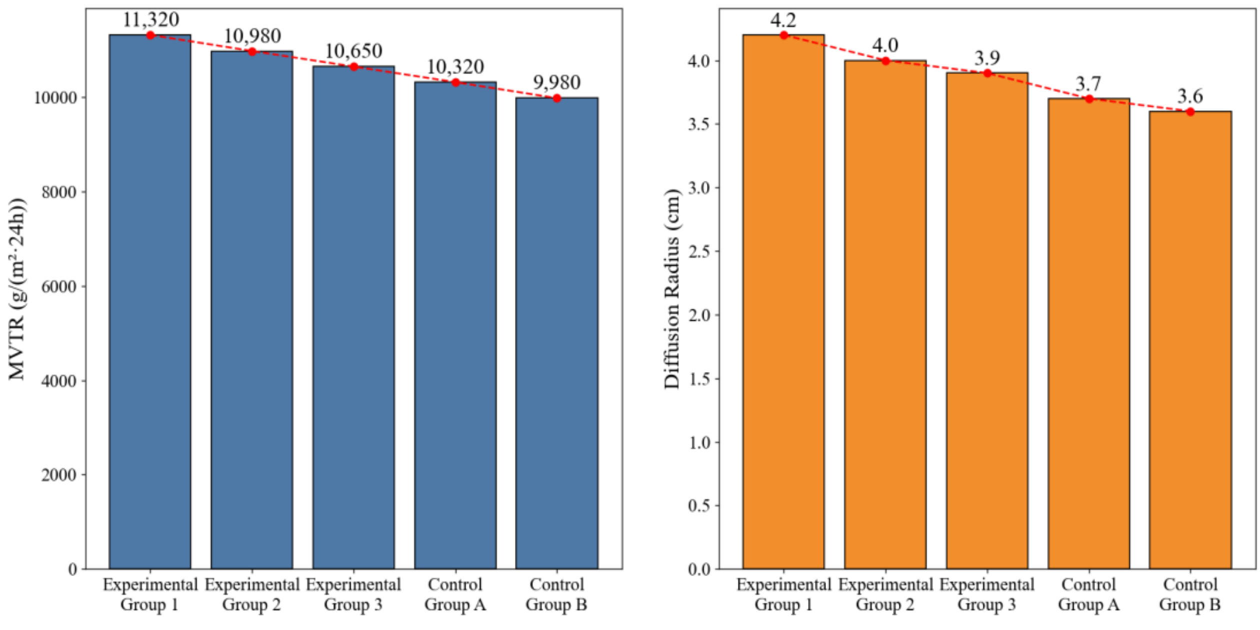

Figure 2. Trends in the moisture vapor transmission rate and moisture diffusion radius of functional fiber fabrics under different spinning conditions

As shown in Figure 2, with increasing spinning temperature and drawing rate, the moisture vapor permeability decreased from 11,320 g/(m²·24 h) in experimental group 1 to 9,980 g/(m²·24 h) in control group B, and the moisture diffusion radius dropped from 4.2 cm to 3.6 cm. Elevated temperature gradients and drawing rates promote phase separation and axial orientation, resulting in a more organized microchannel network and enhanced surface hydrophilicity, which facilitate directional moisture transport despite reduced overall porosity. In contrast, poor parameter control in the control group led to coarser fibers and incomplete microporous structures, which reduced moisture permeability and conductivity. These results confirm the spinning process's effectiveness in regulating the fiber structure and reveal the link between the fiber morphology and thermal–moisture properties, providing an experimental basis for designing high-performance sports textiles.

Elastic Recovery and Fabric Support Performance

To meet football training requirements for fabric elasticity and support, five groups of functional fiber samples were prepared, and their ERR and tension distribution variance (TDV) were measured. The ERR reflects the recovery ability of a fabric after stretching, directly influencing muscle support during movement. The TDV describes the uniformity of stress distribution under load, with lower values indicating more stable tension transmission and better mechanical adaptability. Figure 3 shows the trends of these two indicators with varying spinning parameters.

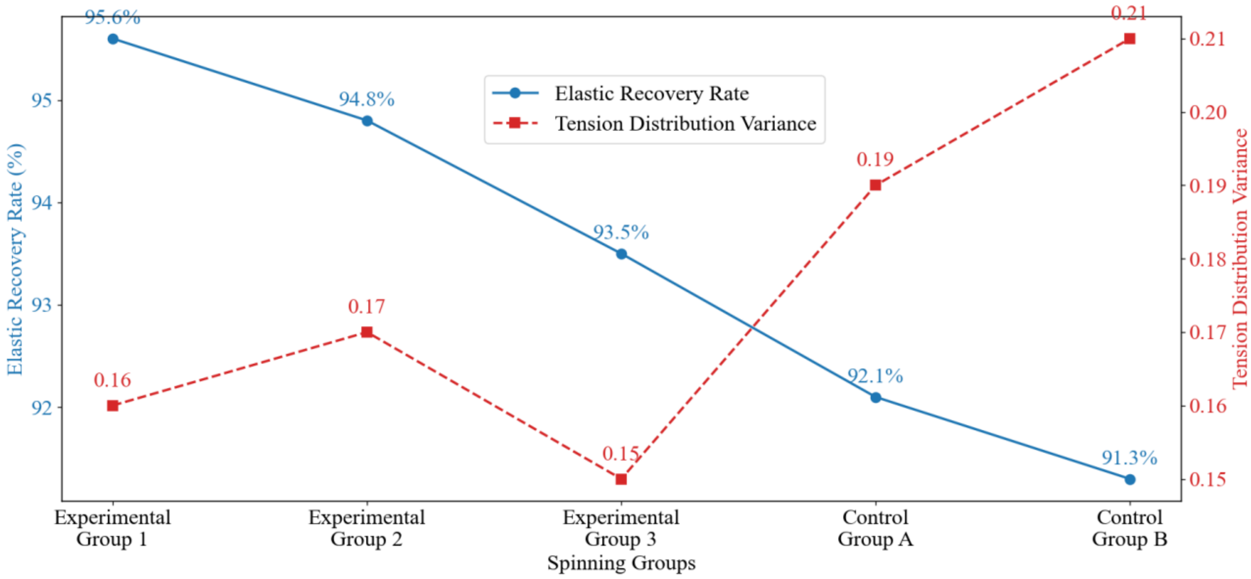

Figure 3. Comparison of the elastic recovery and tensile distribution performance of functional fiber fabrics

As shown in Figure 3, the experimental group outperformed the control group in terms of ERR, reaching 95.6% (experimental group 1) compared with 91.3% in control group B, indicating that the optimized spinning process enhances fiber recovery, likely due to more uniform microchannel distribution and stable two-component bonding. For the tension distribution, the experimental group had lower variance, while control group B showed a high variance of 0.21, suggesting stress concentration that reduced support uniformity. These results demonstrate that regulating spinning temperature difference and drawing rate improves fiber structural uniformity and enhances elastic and mechanical adaptability.

Evaluation Results of Friction Resistance and Wearing Comfort

In football training, sportswear must meet the different friction and comfort needs of various body parts. This study developed a fabric with a microporous structure and surface lubrication by adjusting the spinning process and systematically tested the local COF and subjective comfort scores of key areas during each training stage. COF indicates the sliding resistance between the fabric and the skin, reflecting smoothness and sport adaptability, whereas the subjective score captures overall wearing comfort. Data were collected from four typical areas (upper back, lower thigh, knee, and upper arm) at the beginning, middle, and end of training to analyze the correlation between friction performance and comfort. Figure 4 illustrates the changing trends of both indicators throughout training.

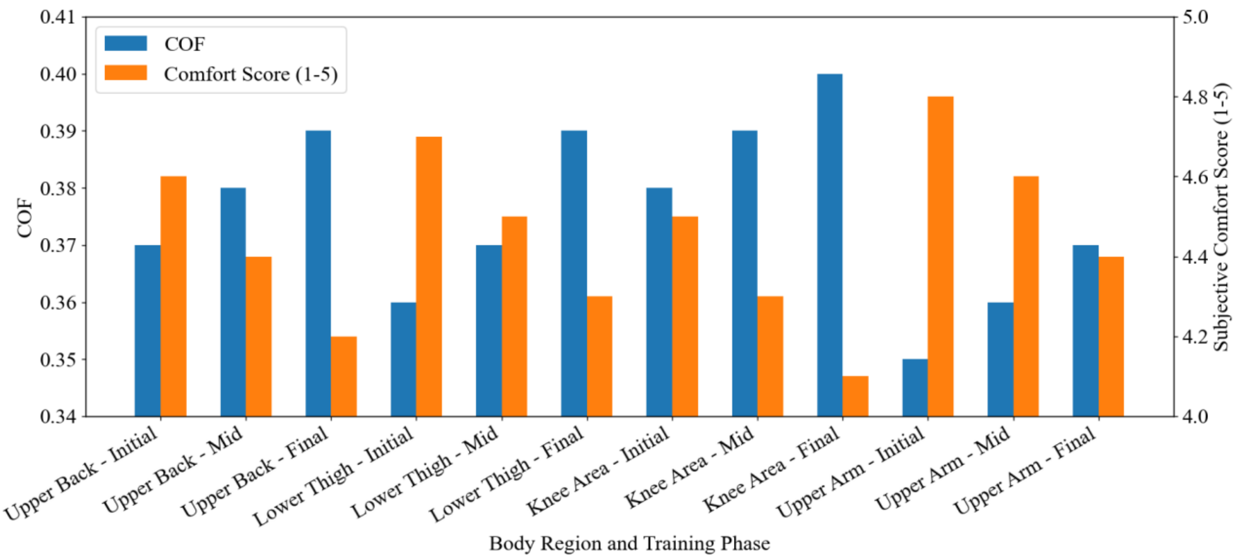

Figure 4. Comparison of local COF and subjective comfort score in different body parts and training stages

As shown in Figure 4, the friction coefficient of each part increased during training, while the subjective comfort score decreased. The knee area showed the highest friction coefficient at the end (0.40), with the comfort score dropping to 4.1, indicating that repeated flexion and extension increased friction and reduced comfort. In contrast, the upper arm maintained a low friction coefficient (minimum 0.35) and a comfort score above 4.4, reflecting a lower friction coefficient maintained throughout dynamic motion and a better fit. This difference relates to the physiological and sports characteristics of each part: the upper arm has high movement frequency but small contact area, and the fabric's microporous structure and surface treatment help reduce friction; the knee undergoes large shear and tensile deformation, easily affecting structural flatness. Increased training intensity and sweating further enhance fabric-skin interface effects, raising the friction coefficient and reducing comfort. These results verify the effectiveness of functional fiber materials in local friction control and support structural optimization of high-performance sportswear.

Changes in Skin Temperature and Humidity Environment during Training

In football training, thermal and humidity regulation of sportswear is key to maintaining body surface microclimate stability. To assess the designed clothing's adaptability to skin temperature and humidity, data were collected from three typical body parts—upper back, outer thigh, and upper arm—at different training stages (beginning, middle, end, recovery). The upper back, with dense sweat glands and poor ventilation, represents heat and moisture buildup; the outer thigh reflects elasticity and local breathability; the upper arm indicates the fabric’s moisture conduction and evaporation efficiency. Analyzing temperature and humidity trends reveals the microenvironment regulation mechanism of functional fibers during dynamic training. Figure 5 shows the changes in skin temperature and humidity throughout the training cycle.

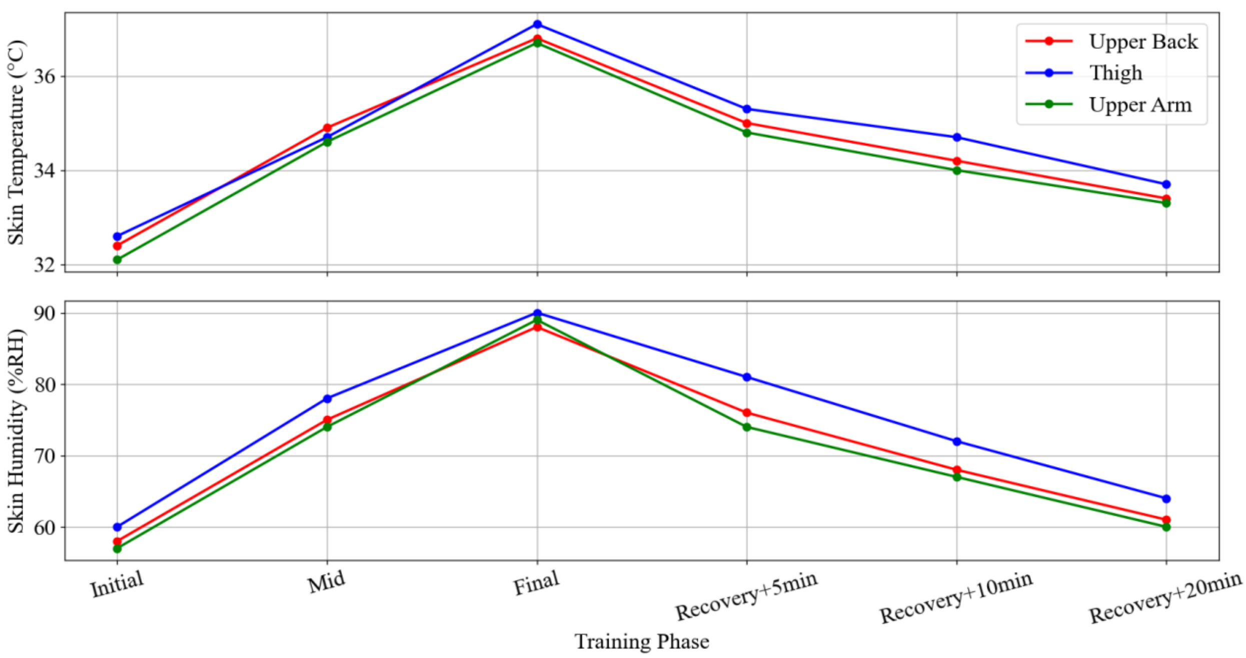

Figure 5. Trends in skin temperature and humidity of various body parts during different training phases and recovery periods

As shown in Figure 5, the skin temperature of the three main body parts rose during training, peaking at the end (highest: 37.1 °C on the outer thigh) due to high metabolism and muscle load. The upper arm heated up and cooled down rapidly, reflecting good air exchange, while the upper back showed continuous heating and slow recovery, with clear heat accumulation. For humidity, all parts saw significant increases; the outer thigh reached 90% RH with heavy sweating but limited evaporation. During recovery, the upper arm’s humidity dropped fastest, indicating the best moisture conduction and breathability. These thermal and humidity changes relate to the structure of functional fiber materials: microporous channels enhance moisture diffusion, hydrophilic modification improves moisture conduction, and the elastic structure maintains thermal and humidity regulation even in a fitted state. The results confirm that functional fiber materials based on textile engineering can effectively regulate the skin microclimate during dynamic sports.

Comparison of Heart Rate Response and Fatigue Perception

To evaluate the impact of high-performance sportswear on athletes' heart rate response and fatigue perception during football training, this study analyzes the regulatory effect of functional fiber materials on physiological state by monitoring heart rate and subjective fatigue scores of different body parts (upper back, outer thigh, knee, upper arm) in the initial, middle, and final stages. Heart rate, as a key indicator of cardiovascular load, reflects physiological responses at various training phases; fatigue score, based on athletes' perception, indicates muscle fatigue accumulation.

The progressive increase in heart rate reflects cardiovascular strain under sustained exertion, with slower acceleration indicating reduced thermal strain. Subjective fatigue scores correlate with neuromuscular endurance, where delayed escalation implies preserved motor control. These responses are linked to movement consistency, as stable skin microclimate reduces thermal discomfort and delays fatigue onset. The elastic structure mitigates muscle oscillation, inferred from restrained EMG amplitude rise, supporting joint stability during repetitive high-load actions. Moisture management maintains skin-fabric interface integrity, which is essential for sustained coordination in dynamic tasks.

By comparing heart rate and fatigue score trends across body parts and stages, the effectiveness of functional fibers in reducing fatigue and maintaining physiological stability is revealed. Figure 6 shows changes in heart rate and fatigue scores during training.

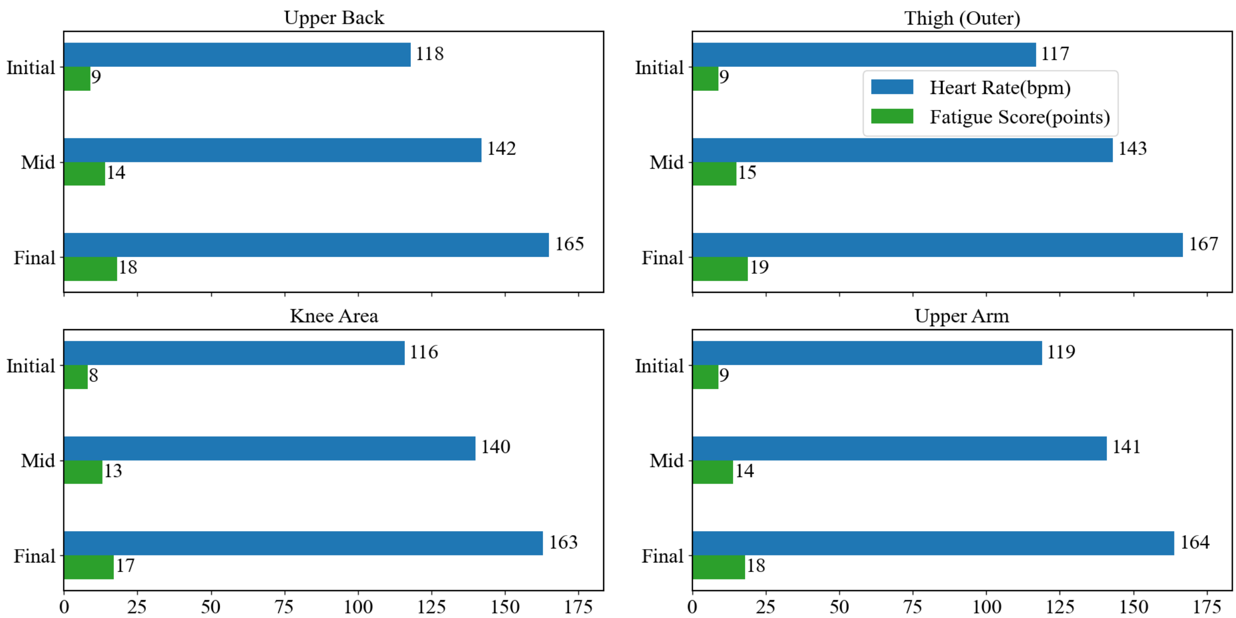

Figure 6. Changes in heart rate and fatigue perception in different body parts during the whole training process

As shown in Figure 6, regardless of body part, heart rate and fatigue score gradually increase as training progresses, indicating that rising intensity leads to greater physiological load and muscle fatigue. In the initial stage, heart rates are low—118 bpm for the upper back and 117 bpm for the outer thigh—with correspondingly low fatigue scores. In the middle stage, heart rate rises significantly to 142 bpm (upper back) and 143 bpm (outer thigh), while fatigue scores increase to 14 and 15 points, respectively. In the final stage, heart rates peak at 165 bpm and 167 bpm, with fatigue scores reaching 18 and 19. This trend aligns with the typical pattern of high-intensity training, where prolonged duration leads to accumulating physiological stress and muscle fatigue.

CONCLUSIONS

This study explores functional fiber materials for high-performance football training apparel and their impact on athletic performance. Using composite spinning and microstructure control, fibers with microporous, multi-component parallel structures were developed and applied in weft-knitted stretch and multilayer composite fabrics. Tests showed that the material achieved a moisture permeability of 11,320 g/(m^2·24 h), a moisture diffusion radius of 4.2 cm, and an elastic recovery of 95.6%, enhancing thermal–moisture management, quick drying, and muscle support. Training results indicate improved skin microclimate, reduced friction, and delayed fatigue. Compared to the control group, the experimental group showed slower increases in skin moisture, fatigue scores, and heart rate fluctuations. A limitation remains: the knee area's friction coefficient (COF) reached 0.40, which negatively impacted comfort.

Current validation utilized a limited athlete cohort, constraining applicability across diverse physiological profiles. Laboratory-based training scenarios fail to capture the unpredictability of real match dynamics with variable environmental conditions. Long-term performance degradation after repeated laundering cycles remains unquantified, creating uncertainty about sustained functionality. Future investigations may expand to multicenter studies with broader demographic representation. Rigorous assessment of material stability through standardized washing protocols is essential to define service life expectations. Targeted modification of high-friction zones like knee articulations requires focused development to balance structural resilience with movement efficiency. Integration of antimicrobial properties without compromising thermal regulation warrants systematic exploration. Determining the performance envelope under extreme environmental conditions will validate global applicability across diverse climatic zones and will help optimize surface treatments to reduce local friction and incorporate antibacterial and antistatic functionalities, further improving adaptability and performance of sportswear.

Author Contributions

All work in this study was independently completed by Lei WANG.

Human Research Subjects

This study was approved by the Ethics Committee of Inner Mongolia University of Finance and Economics. All participants provided informed consent prior to the study.

Conflicts of Interest

The author declares no conflict of interest.

Funding

This research received no external funding.

Acknowledgements

Not applicable.

REFERENCES

[1] Saravanja A, Pusic T, Volmajer Valh J, Dekanić T. Aging and Modified Washing Process for Polyester Fabrics—Environmental Impact. Polymers. 2024; 16(23):3238-3257. doi: 10.3390/polym16233238

[2] Nasrin S, Mandal S, Islam MDM, Petrova A, Agnew RJ, Boorady LM. Factors affecting the sweat-drying performance of active sportswear—A review. Textiles. 2023; 3(3):319-338. doi: 10.3390/textiles3030022

[3] Kim HA. Moisture vapor permeability and thermal wear comfort of ecofriendly fiber-embedded woven fabrics for high-performance clothing. Materials. 2021; 14(20):6205-6229. doi: 10.3390/ma14206205

[4] Xiao YQ, Kan CW. Review on the development and application of directional water transport textile materials. Coatings. 2022; 12(3):301-318. doi: 10.3390/coatings12030301

[5] Cheng P. Investigation of the impact of movement speed on the comprehensive comfort of tight-fitting sportswear. Journal of Industrial Textiles. 2025; 55:15280837251339678-15280837251339698. doi: 10.1177/15280837251339678

[6] Shak Sadi M, Kumpikaite E. Advances in the robustness of wearable electronic textiles: Strategies, stability, washability and perspective. Nanomaterials. 2022; 12(12):2039-2086. doi: 10.3390/nano12122039

[7] Fu C, Xu X, Yin GZ, Xu B, Li P, Ai B, et al. Surface engineering for cellulose as a boosted Layer-by-Layer assembly: excellent flame retardancy and improved durability with introduction of bio-based "molecular glue". Applied Surface Science. 2022; 585:152550-152587. doi: 10.1016/j.apsusc.2022.152550

[8] Atalie D, Tesinova P, Tadesse MG, Ferede E, Dulgheriu I, Loghin E. Thermo-physiological comfort properties of sportswear with different combination of inner and outer layers. Materials. 2021; 14(22):6863-6875. doi: 10.3390/ma14226863

[9] Chen C, Feng J, Li J, Guo Y, Shi X, Peng H. Functional fiber materials to smart fiber devices. Chemical Reviews. 2022; 123(2):613-662. doi: 10.1021/acs.chemrev.2c00192

[10] Atallah HAA, Saleh YDM, Glal El-Den RE, Abdel Wahab SSM, Hassabo AG. Importance of Thermal Insulation in Sportswear Design. Journal of Textiles, Coloration and Polymer Science. 2025; 22(2):59-64. doi: 10.21608/jtcps.2024.259733.1312

[11] Dolez PI, Marsha S, McQueen RH. Fibers and textiles for personal protective equipment: review of recent progress and perspectives on future developments. Textiles. 2022; 2(2):349-381. doi: 10.3390/textiles2020020

[12] Gulati R, Sharma S, Sharma RK. Antimicrobial textile: Recent developments and functional perspective. Polymer Bulletin. 2022; 79(8):5747-5771. doi: 10.1007/s00289-021-03826-3

[13] Ioannou LG, Tsoutsoubi L, Gkiata P, Brown HA, Periard JD, Mekjavic IB, et al. Effect of sportswear on performance and physiological heat strain during prolonged running in moderately hot conditions. Scandinavian Journal of Medicine & Science in Sports. 2024; 34(1):e14520-e14533. doi: 10.1111/sms.14520

[14] Zhao X, Li M, Zhao J, Wang X. Intelligent sportswear design: Innovative applications based on conjugated nanomaterials. Science and Engineering of Composite Materials. 2024; 31(1):20240032-20240050. doi: 10.1515/secm-2024-0032

[15] Cheng P, Zeng X. Investigation into the dynamic change mechanism of comfort perception in tight-fitting sportswear during physical activity. Journal of Industrial Textiles. 2025; 55:15280837251321856-15280837251321878. doi: 10.1177/15280837251321856

[16] Wei HT, Chan WS, Chow DHK. Systematic review of selecting comfortable sportswear: Predicting wearing comfort based on physiological responses and materials properties. Textile Research Journal. 2023; 93(15-16):3926-3941. doi: 10.1177/00405175231167863

[17] Gadeikyte A, Abraitienė A, Barauskas R. Prediction of air permeability coefficient and water-vapor resistance of 3D textile layer. The Journal of The Textile Institute. 2022; 113(3):396-404. doi: 10.1080/00405000.2021.1883237

[18] Adamu BF, Gao J. Comfort related woven fabric transmission properties made of cotton and nylon. Fashion and Textiles. 2022; 9(1):8-18. doi: 10.1186/s40691-021-00285-2

[19] Gorji M, Mazinani S, Gharehaghaji AA. A review on emerging developments in thermal and moisture management by membrane-based clothing systems towards personal comfort. Journal of Applied Polymer Science. 2022; 139(27):e52416-e52443. doi: 10.1002/app.52416

[20] Islam MR, Golovin K, Dolez PI. Clothing thermophysiological comfort: A textile science perspective. Textiles. 2023; 3(4):353-407. doi: 10.3390/textiles3040024

[21] Cui G, Wang C. Applications and development trends of textile materials in sports: A review. Alexandria Engineering Journal. 2025; 126:491-506. doi: 10.1016/j.aej.2025.04.094

[22] Guo N, Li Z, Chen N, Dai H, Liu K, Zhang P. Optimization design of functional running pants and evaluation of thermal-humid comfort capabilities. Textile Research Journal. 2024; 94(3-4):415-426. doi: 10.1177/00405175231196323

[23] Hassabo AG, Eid MM, Mahmoud ER, Asser NA. Innovation of smart knitted fabrics for functional performance of sportswear upon treatment using phase change material. Egyptian Journal of Chemistry. 2023; 66(3):133-156. doi: 10.21608/ejchem.2023.194982.7623

[24] Cheng P, Wang J, Zeng X, Bruniaux P, Tao X. Intelligent research on wearing comfort of tight sportswear during exercise. Journal of Industrial Textiles. 2022; 51(3_suppl):5145S-5168S. doi: 10.1177/15280837221094055

[25] Baik K, Yoon SY, Lee S, Park CH. Deformation recovery and dimensional stability properties of fabrics in a clothing care machine. Fibers and Polymers. 2023; 24(4):1453-1462. doi: 10.1007/s12221-023-00039-5

[26] Wan A, Xu T, Wang X, Hao G. Effect of Yarn Characteristics on Bagging Recovery and Comfort Properties of Warp-Knitted Fabric for Sport and Recreation. Fibers and Polymers. 2025; 26(3):1411-1421. doi: 10.1007/s12221-025-00864-w

[27] Cubric I S, Cubric G, Matkovic VMP, Cuden AP. The comfort of knitted fabrics: interaction of sportswear and athlete’s body. Communications in Development and Assembling of Textile Products. 2021; 2(1):70-79. doi: 10.25367/cdatp.2021.2

[28] Ahmad F, Akhtar KS, Anam W, Mushtaq B, Rasheed A, Ahmad S, et al. Recent developments in materials and manufacturing techniques used for sports textiles. International Journal of Polymer Science. 2023; 2023(1):2021622-2021642. doi: 10.1155/2023/2021622